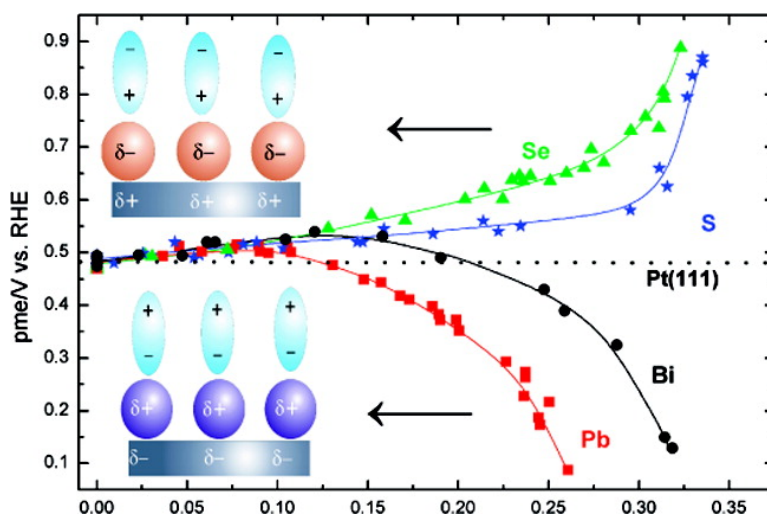


## Evidence of Water Reorientation on Model Electrocatalytic Surfaces from Nanosecond-Laser-Pulsed Experiments

Nuria Garca-Arez, Vctor Climent, and Juan M. Feliu

*J. Am. Chem. Soc.*, **2008**, 130 (12), 3824-3833 • DOI: 10.1021/ja0761481

Downloaded from <http://pubs.acs.org> on February 8, 2009



### More About This Article

Additional resources and features associated with this article are available within the HTML version:

- Supporting Information
- Access to high resolution figures
- Links to articles and content related to this article
- Copyright permission to reproduce figures and/or text from this article

[View the Full Text HTML](#)

## Evidence of Water Reorientation on Model Electrocatalytic Surfaces from Nanosecond-Laser-Pulsed Experiments

Nuria García-Aráez, Víctor Climent,\* and Juan M. Feliu

*Instituto de Electroquímica, Universidad de Alicante, Ap. 99, E-03080, Alicante, Spain*

Received August 15, 2007; E-mail: victor.climent@ua.es

**Abstract:** The behavior of water at the interface formed between a quasi-perfect Pt(111) single-crystal electrode and an aqueous electrolyte solution is studied by means of the laser-induced temperature jump method. This method is based on the use of nanosecond laser pulses to suddenly increase the temperature at the interface. The measurement of the response of the interface toward the laser heating under coulstatic conditions provides evidence on the net orientation of water at the interface. Especially interesting is the study of the effect on the interfacial water caused by the selective deposition of foreign metal adatoms, because these bimetallic systems usually exhibit appealing electrocatalytic properties. The T-jump methodology shows that the surface composition strongly affects the interaction of water with the surface. The most representative parameter to characterize this interaction is the potential where water reorientation occurs; this potential shifts in different directions, depending on the relative values of the electronegativity of the adatom and the substrate. These results are discussed in the light of available information about the effect of adatom deposition on the work function and the surface potential of the modified surface. Finally, some implications on the enhancement of the electrocatalytic activity are briefly discussed.

### 1. Introduction

The development of new electrocatalytic materials by deposition of foreign adatoms on a host metal has been a central subject of study in electrochemistry during the last 30 years.<sup>1–3</sup> The interest in the field of bimetallic catalysts has been renewed recently, given the necessity of finding suitable electrode materials for operative fuel cells.<sup>4–7</sup> In this regard, most of the efforts have been focused on platinum as a substrate, because of the very high reactivity of this metal for fuel-cell reactions. Still, a surface modifier is necessary to improve the catalytic activity and stability of the electrode and to avoid poisoning side reactions. It has been shown that the modification of platinum surfaces with submonolayer amounts of elements of the p-block of the periodic table leads, in many cases, to electrode materials with greatly improved catalytic properties.<sup>1,2,8</sup> Furthermore, from a fundamental point of view, the study and characterization of bimetallic surfaces can provide a deeper understanding of the general phenomena of electrocatalysis, leading to a rational schema for the design and development of

new electrocatalytic materials.<sup>7,9</sup> In this regard, three main effects are usually invoked to explain the catalytic enhancement: the electronic (ligand) effect, which is associated with changes in the electronic properties of the substrate; the ensemble (geometrical) effect, which is related to changes in the occupancy of adsorption sites of a given geometry; and the bifunctional effect, where the surface species provides one of the necessary reactant sites. Although the separation of these effects is usually difficult,<sup>8,10</sup> it will be shown that the method presented here provides valuable information on the electronic and geometric effects that are associated to adatom deposition. Finally, it is important to stress that, given the paramount importance of the surface structure on the electrocatalytic activity, the use of a quasi-perfect Pt(111) single-crystal electrode is required in this type of fundamental study.

Among the different ways to modify the surface of noble-metal electrodes, the irreversible adsorption method deserves special attention (see, for example, refs 11–14). Irreversible adsorption occurs when the adatom adlayer remains adsorbed on the surface of the host metal in a wide potential range (typically from 0 to 0.7–1.0 V vs a reversible hydrogen electrode (RHE)), despite the fact that the solution does not contain ions of the adatom that could be in equilibrium with

- (1) Parsons, R.; VanderNoot, T. *J. Electroanal. Chem.* **1988**, *257*, 9–45.
- (2) Jarvi, T. D.; Stuve, E. M. In *Electrocatalysis*; Lipkowsky, J., Ross, P. N., Eds.; Wiley-VCH: New York, 1998; pp 75–153.
- (3) Feliu, J. M.; Herrero, E. In *Handbook of Fuel Cells—Fundamentals, Technology and Applications*; Vielstich, W., Gasteiger, H., Lamm, A., Eds.; Wiley: New York, 2003.
- (4) Zhang, J.; Sasaki, K.; Sutter, E.; Adzic, R. R. *Science* **2007**, *315*, 220–222.
- (5) Casado-Rivera, E.; Gal, Z.; Angelo, A. C. D.; Lind, C.; DiSalvo, F. J.; Abruna, H. D. *Chem. Phys. Chem.* **2003**, *4*, 193–199.
- (6) Stamenkovic, V. R.; Fowler, B.; Mun, B. S.; Wang, G. F.; Ross, P. N.; Lucas, C. A.; Markovic, N. M. *Science* **2007**, *315*, 493–497.
- (7) Stamenkovic, V.; Mun, B. S.; Mayrhofer, K. J. J.; Ross, P. N.; Markovic, N. M.; Rossmeisl, J.; Greeley, J.; Nørskov, J. K. *Angew. Chem., Int. Ed.* **2006**, *45*, 2897–2901.
- (8) Leiva, E.; Iwasita, T.; Herrero, E.; Feliu, J. M. *Langmuir* **1997**, *13*, 6287–6293.

- (9) Greeley, J.; Jaramillo, T. F.; Bonde, J.; Chorkendorff, I. B.; Nørskov, J. K. *Nat. Mater.* **2006**, *5*, 909–913.
- (10) Liu, P.; Nørskov, J. K. *Phys. Chem. Chem. Phys.* **2001**, *3*, 3814–3818.
- (11) Clavilier, J.; Feliu, J. M.; Aldaz, A. *J. Electroanal. Chem.* **1988**, *243*, 419–433.
- (12) Clavilier, J.; Orts, J. M.; Feliu, J. M.; Aldaz, A. *J. Electroanal. Chem.* **1990**, *293*, 197–208.
- (13) Feliu, J. M.; Fernandez-Vega, A.; Orts, J. M.; Aldaz, A. *J. Chim. Phys. Phys.-Chim. Biol.* **1991**, *88*, 1493–518.
- (14) Feliu, J. M.; Gómez, R.; Llorca, M. J.; Aldaz, A. *Surf. Sci.* **1993**, *289*, 152–162.

the adsorbed species. This has the clear advantage that the adatom coverage is not dependent on the applied potential (within the stability potential range) and, hence, it can be varied independently in a continuous way. The irreversible adsorption is experimentally very convenient, because the modification is achieved by just dipping the electrode in a solution that contains the corresponding ion. The electrode modified with the adlayer created in this way can be rinsed and transferred to the electrochemical cell. During this process, surface contamination should be maintained below the level of detection.

On the other hand, the importance of the role that water has in many electrocatalytic processes is evidenced by the striking differences in reactivity that are observed in gas-phase heterogeneous catalysis and electrocatalysis. This subject is especially relevant within the context of fuel-cell technology, where the oxidation of CO and small organic molecules involves water adsorption and dissociation steps.<sup>2,15,16</sup> Besides, in other situations, surface water or its dissociation products have been postulated to act as inhibitors, blocking necessary sites for the electrochemical reaction.<sup>17–20</sup> However, despite its importance, the role that water molecules have in electrochemical reactions is poorly understood. One of the main difficulties in the study of interfacial water is the interference of its response from that of water in the bulk of the solution. In this regard, the laser-induced temperature jump method allows one to study the behavior of interfacial water selectively.<sup>21–25</sup> This technique was previously used by Benderskii et al.<sup>21</sup> with mercury electrodes, as well as by Smalley et al.<sup>26</sup> with polycrystalline platinum. Another big advantage of this technique is the possibility of decoupling the charge-transfer process that is associated with adsorption phenomena from the purely double-layer response, by making the temperature jump sufficiently fast.<sup>22</sup> The response of the electrode potential to the change of the temperature gives a measure of the temperature coefficient of the double-layer potential. This coefficient is related with the entropy of formation of the double layer: the potential where this coefficient becomes zero corresponds to the potential of maximum entropy (pme) of formation of the double layer.<sup>21,27</sup> Furthermore, as will be discussed below, the importance of the pme as a fundamental parameter characterizing the interface stems from the fact that it can be identified with the potential of turnover of the interfacial water network.

As a result of the electrostatic interaction of the water dipoles with the electric field at the interface, the potential of water

reorientation will be closely related to the potential of zero charge ( $E_{pzc}$ ). Thus, for a negatively charged surface, we can expect the water molecules to be polarized with the positive end closer to the metal, whereas the opposite is true when the surface is positively charged. Indeed, the reorientation of water induced by the electrode potential has been identified spectroscopically in a limited number of situations.<sup>28</sup> However, it should be noted that this picture is complicated by the existence of a chemical interaction between the water and the metal surface, which has a tendency to orientate the water molecules, even in the absence of any electric field. This natural orientation is with the oxygen closer to the metal surface in the case of gold<sup>23,29</sup> and mercury<sup>21,27,30</sup> electrodes; as a result, the potential of water reorientation is located at slightly negative charge densities. The decrease of the work function upon water dosage supports the same picture for Pt(111).<sup>31</sup>

The importance of the  $E_{pzc}$  as a key parameter to understand the electrochemical reactivity has often been emphasized. In this regard, it is expected that the  $E_{pzc}$  of an adatom-modified surface will be dependent on the adatom coverage, as a result of the surface dipole induced by the adatom adsorption. Unfortunately, the  $E_{pzc}$  of adatom-modified platinum single-crystal electrodes is not available, because the different methods that have been used for the indirect determination of this parameter are not suitable in the presence of adatoms. The lack of information about the  $E_{pzc}$  of adatom-modified surfaces can, in part, be palliated with the knowledge provided from the study of the variation of the pme, because this study provides insight on the direction of the surface dipole induced by the adatom deposition, and also on the specific interactions of the water molecules with the metal surface. This method has been applied to the study of Au(111),<sup>23</sup> Pt(111),<sup>22</sup> Pt(111) stepped surfaces,<sup>24</sup> and Bi–Pt(111)<sup>25</sup> single-crystal electrodes. In the present paper, we will extend this study to Pt(111) that has been modified by lead, selenium, and sulfur deposition, and Pt(111) stepped surfaces modified by bismuth deposition. It will be shown that the method proposed here provides valuable information on the fundamental properties of bimetallic surfaces and gives insight on some relevant implications in catalysis.

## 2. Experimental Section

The Pt(111) electrode was prepared following Clavilier's procedure.<sup>32</sup> The electrode was oriented, cut, and polished from single-crystal platinum beads, which were obtained by the melting and subsequent slow crystallization of a 99.999% platinum wire (Goodfellow Metals and Johnson Matthey). The orientation procedure took advantage of the reflection of visible light on the (111) and (100) facets grown naturally on the bead surface, which can be seen correctly only when the bead is really a single crystal. The bead was fixed at the center of a four rotation goniometer head that was placed at the end of an optical bench. The dimensions of the bench (1.5 m) and the control of the reflected light from the polished sample enable a precision in the orientation of approximately  $\pm 3$  minutes of arc. In this way, most macroscopic surface imperfections should be attributed to the final polishing step, prior to the annealing of the surface. This final polishing

(15) Shiroishi, H.; Ayato, Y.; Kunimatsu, K.; Okada, T. *J. Electroanal. Chem.* **2005**, *581*, 132–138.

(16) Franaszczuk, K.; Herrero, E.; Zelenay, P.; Wieckowski, A.; Wang, J.; Masel, R. I. *J. Phys. Chem.* **1992**, *96*, 8509–8516.

(17) Iwasita, T.; Xia, X. H.; Liess, H. D.; Vielstich, W. *J. Phys. Chem. B* **1997**, *101*, 7542–7547.

(18) Climent, V.; Attard, G. A.; Feliu, J. M. *J. Electroanal. Chem.* **2002**, *532*, 67–74.

(19) Wang, J. X.; Markovic, N. M.; Adzic, R. R. *J. Phys. Chem. B* **2004**, *108*, 4127–4133.

(20) Climent, V.; Macia, M. D.; Herrero, E.; Feliu, J. M.; Petrii, O. A. *J. Electroanal. Chem.* **2008**, *612*, 269–276.

(21) Benderskii, V. A.; Velichko, G. I. *J. Electroanal. Chem.* **1982**, *140*, 1–22.

(22) Climent, V.; Coles, B. A.; Compton, R. G. *J. Phys. Chem. B* **2002**, *106*, 5988–5996.

(23) Climent, V.; Coles, B. A.; Compton, R. G. *J. Phys. Chem. B* **2002**, *106*, 5258–5265.

(24) Climent, V.; Coles, B. A.; Compton, R. G.; Feliu, J. M. *J. Electroanal. Chem.* **2004**, *561*, 157–165.

(25) Climent, V.; Garcia-Araez, N.; Compton, R. G.; Feliu, J. M. *J. Phys. Chem. B* **2006**, *110*, 21092–21100.

(26) Smalley, J. F.; Krishnan, C. V.; Goldman, M.; Feldberg, S. W.; Ruzic, I. *J. Electroanal. Chem.* **1988**, *248*, 255–282.

(27) Harrison, J. A.; Randles, J. E. B.; Schiffrin, D. J. *J. Electroanal. Chem.* **1973**, *48*, 359–381.

(28) Henderson, M. A. *Surf. Sci. Rep.* **2002**, *46*, 1–308.

(29) Silva, F.; Sottomayor, M. J.; Hamelin, A. *J. Electroanal. Chem.* **1990**, *294*, 239–251.

(30) Trasatti, S. *J. Electroanal. Chem.* **1977**, *82*, 391–402.

(31) Villegas, I.; Weaver, M. J. *J. Phys. Chem.* **1996**, *100*, 19502–19511.

(32) Clavilier, J.; Armand, D.; Sun, S.-G.; Petit, M. *J. Electroanal. Chem.* **1986**, *205*, 267–277.

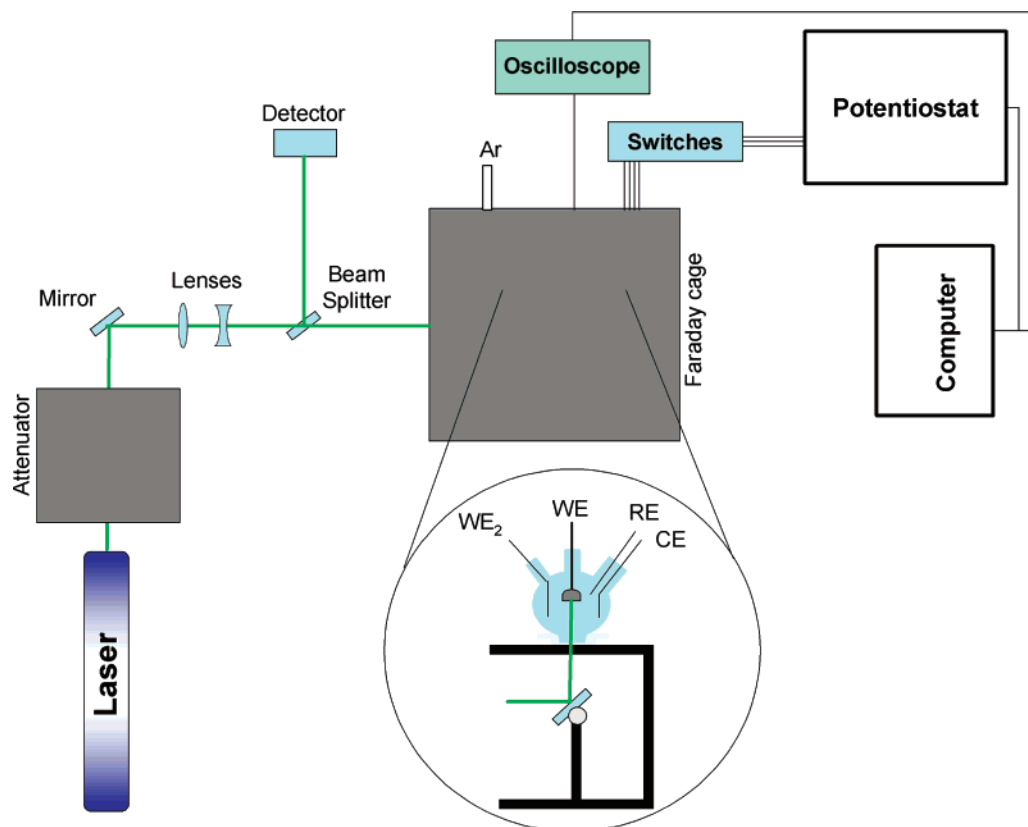


Figure 1. Sketch of the experimental setup for the laser experiments.

was achieved using  $0.25\ \mu\text{m}$  diamond paste and the final annealing was made at  $\sim 1100\ ^\circ\text{C}$  for several minutes.

Prior to each experiment, the electrode was annealed in a Bunsen flame (propane-air), cooled down in a flow of  $\text{H}_2/\text{Ar}$  (N-50, Air Liquide in all gases used), and protected with a drop of ultrapure water that was in equilibrium with the  $\text{H}_2/\text{Ar}$  gas mixture. A coiled platinum wire was used as a counterelectrode and a hydrogen-charged Pd wire immersed in the working solution was used as a reference electrode. However, all potentials were converted to the RHE scale and are quoted against this reference in the text. Cyclic voltammograms were recorded using a computer-controlled  $\mu$ -Autolab III potentiostat (Eco-Chemie, Utrecht, The Netherlands) under the current integration mode. Solutions were prepared from concentrated  $\text{HClO}_4$  (Merck, suprapur) and  $\text{KClO}_4$  (Merck, p.a.) diluted in ultrapure water ( $18.2\ \text{M}\Omega\ \text{cm}$ ) obtained from an Elgastat water purification system. The  $\text{KClO}_4$  was purified by recrystallization, and the  $\text{HClO}_4$  was used as received. Adatom adsorption was performed by immersion of the electrode in solution prepared from  $\text{Bi}_2\text{O}_3$  (Merck, extra pure),  $\text{PbCO}_3$  (Aldrich, ACS Reagent),  $\text{SeO}_2$  (Merck, 99.999%), and  $\text{Na}_2\text{S}$  (Aldrich, Reagent Plus). Different coverages were obtained by varying the adatom concentration and/or the exposure time. The electrode was then rinsed with ultrapure water and introduced into an electrochemical cell that contained a  $0.1\ \text{M}$   $\text{KClO}_4 + 1\ \text{mM}$   $\text{HClO}_4$  supporting electrolyte solution. For the case of lead deposition, the electrode was rinsed with water in equilibrium with the  $\text{H}_2/\text{Ar}$  mixture, to avoid the adatom desorption at the open-circuit potential. The electrolytes were purged with argon, and the solution was kept under an argon blanket throughout the duration of the experiment.

The laser-induced potential transients were recorded as previously explained.<sup>25</sup> Briefly, after recording a voltammogram to ensure the surface order and cleanliness of the solution, the electrode is polarized at a given potential. A fourth platinum electrode is immersed in the cell and polarized exactly at the same potential as the working electrode. Approximately  $200\ \mu\text{s}$  before the laser was fired, both electrodes were

disconnected from the potentiostat and the potential difference between them was measured with a fast differential amplifier. The experiment was repeated at a frequency of  $10\ \text{Hz}$ , which allowed the temperature to relax to its ambient value between consecutive pulses. The potentiostat is reconnected between successive laser pulses, ensuring that the potential is kept at the desired value. Either 128 or 256 potential transients were averaged at each potential, using a Tektronix Model TDS 3054B oscilloscope. After the laser transients were recorded at different potentials, a new voltammogram was recorded and compared to the initial one, to test the stability of the surface in the entire experiment. Only those experiments in which the charge on the final voltammogram was no more than 5% less than the initial one were kept as meaningful.

The light source used was a Brilliant Q-switched Nd:YAG laser (Quantel) operating in frequency-doubled mode at a wavelength of  $532\ \text{nm}$  and pulse duration of  $5\ \text{ns}$ . The beam diameter obtained directly at the laser output is ca.  $6\ \text{mm}$ , and this was reduced to ca.  $4\ \text{mm}$  (slightly bigger than the electrode) by passing it through a conventional arrangement of lenses. The energy of the laser beam is reduced by combining the effect of an attenuator from Newport Corporation (Model M-935-10) and the regulation of the Q-switch delay time. The laser energy is measured with a piezoelectric sensor head (Model LM-P10i), in conjunction with a FieldMaster GS console from Coherent. A laser energy of ca.  $1\ \text{mJ}$  per pulse (i.e.,  $8\ \text{mJ}/\text{cm}^2$ ) was used in all the experiments; this value is well below the damage threshold of the electrode surface. Optics housings, lenses, and mirrors were supplied by Newport Corporation. The experimental setup is depicted in Figure 1.

### 3. Results

Figure 2 shows some cyclic voltammograms (CVs) that correspond to a Pt(111) electrode modified by the adsorption of lead, bismuth, selenium, and sulfur at an intermediate

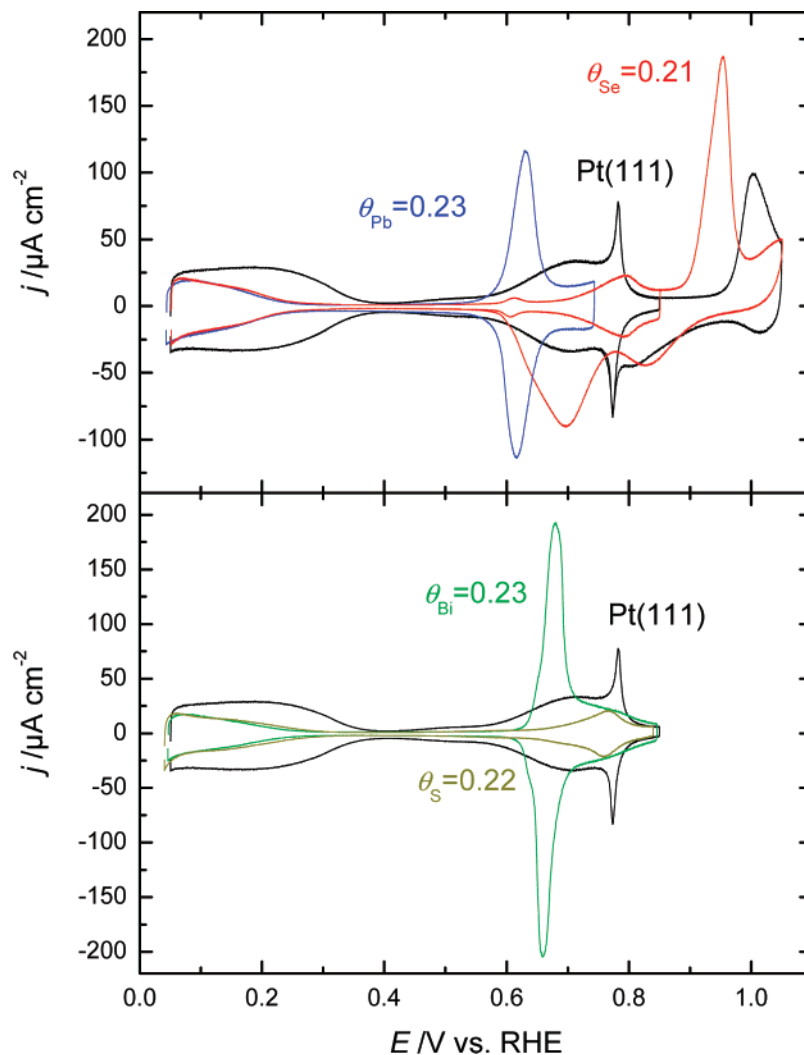


**Figure 2.** Cyclic voltammograms (CVs) of a Pt(111) electrode modified by bismuth, lead, selenium, and sulfur deposition with  $\theta \approx 0.2$  in a 0.1 M  $\text{KClO}_4$  + 1 mM  $\text{HClO}_4$  solution. The CV that corresponds to the unmodified surface is also included, for comparison purposes. Sweep rate = 50 mV/s.

coverage of  $\theta \approx 0.2$  in a 0.1 M  $\text{KClO}_4$  + 1 mM  $\text{HClO}_4$  solution. The CV of the bare Pt(111) electrode is included for comparison. The solution composition was selected, on the one hand, to minimize anion-specific adsorption. On the other hand, the higher pH of this mixture of perchloric/perchlorate solution, in comparison to the more-conventional 0.1 M  $\text{HClO}_4$ , has several advantages for the interpretation of the laser-induced transients, because it minimizes the contributions of kinetics of hydrogen adsorption and the thermodiffusion (Soret) potential.<sup>22,25</sup> The modification of the surface composition by adatom deposition produces two characteristic effects on the CVs. First, the decrease of the current density associated to H and OH adsorption on the free platinum sites in the low- and high-potential regions, respectively. The second effect is the appearance of characteristic peaks that can be attributed to the oxidation/reduction of the adatoms.<sup>11–14</sup>

Previous studies on adatom-modified Pt(111) surfaces in 0.5 M  $\text{H}_2\text{SO}_4$  solutions<sup>11–14</sup> have reported linear relationships between the charge under the adatom redox peaks and the charge corresponding to the noncovered platinum adatoms (calculated from hydrogen and (bi)sulfate adsorption). From the value of the slope, the stoichiometry of the adatom redox processes was inferred. This is  $2e^-/3$  sites for Bi and Pb, and  $4e^-/3$  sites for

Se. According to this interpretation, the adatom coverage can be determined from either the charge under the adatom redox process or from the blockage of hydrogen and/or anion adsorption. However, the stoichiometry of the adatom redox processes in the 0.1 M  $\text{KClO}_4$  + 1 mM  $\text{HClO}_4$  solution used in the present work has only been studied for the case of bismuth deposition.<sup>25</sup> Therefore, it is necessary to first check the applicability of the stoichiometry found in the more-acidic media to the present conditions. For this purpose, the charge that is associated with the adatom redox processes has been plotted as a function of the hydrogen adsorption charge in Figure 3 for the case of Pb and Se deposition. The calculation of the charge values was performed from integration of the voltammograms as explained in ref 25. The linearity of the plots and the value of the slopes confirm the expected stoichiometry.

In conclusion, the coverage of bismuth, lead, and selenium can certainly be calculated from the hydrogen adsorption charge, and the stoichiometries of the reactions have been corroborated in the solution used in the present work. For the case of sulfur, no surface oxidation process has been observed in the available potential window. Moreover, hydrogen adsorption may partially overlap with the reductive desorption of this adatom. Therefore, the OH adsorption charge will be used to calculate the coverage,

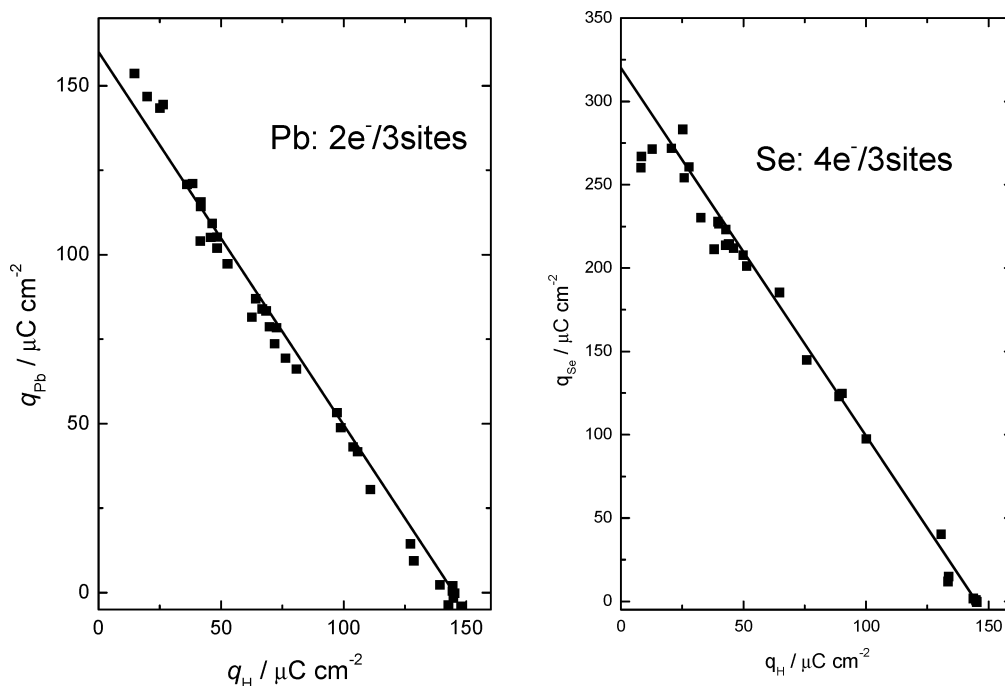


**Figure 3.** Plot of the charge corresponding to the adatom redox process, as a function of the remaining hydrogen charge for a Pt(111) electrode modified by lead and selenium deposition in a 0.1 M  $\text{KClO}_4$  + 1 mM  $\text{HClO}_4$  solution.

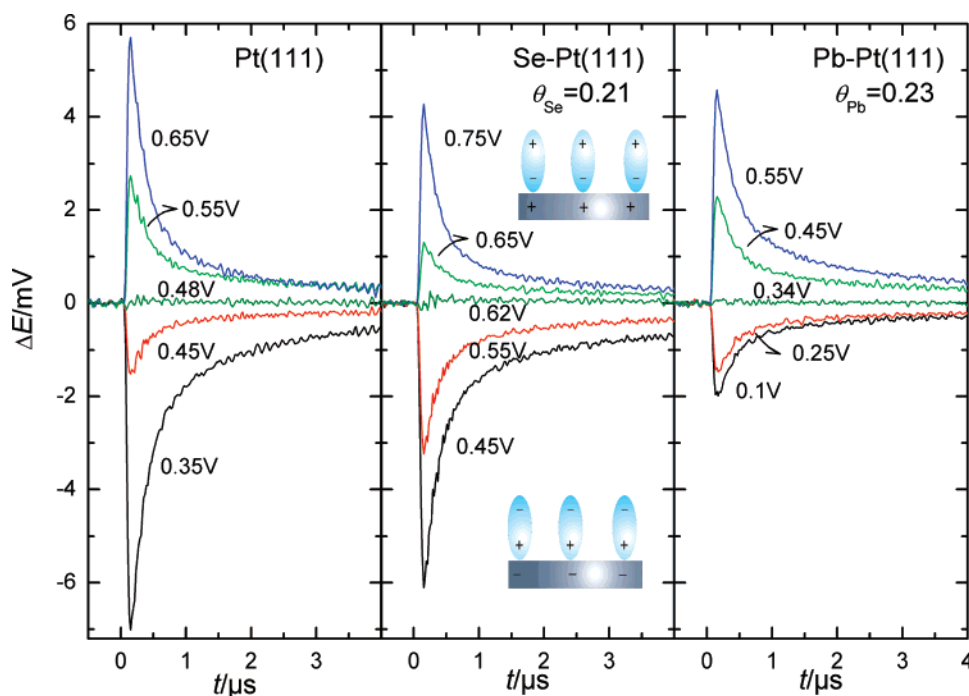


**Figure 4.** Laser-induced coulombic potential transients measured under the same experimental conditions used in Figure 2 for the bare, Se-modified, and Pb-modified Pt(111), at selected potentials, measured vs RHE, as labeled in the figure. The illustrations show the schematic interpretation for the meaning of the potential transients.

assuming a blockage of three platinum sites, as suggested by the maximum coverage of 0.33 reported elsewhere.<sup>33</sup>

The general behavior of the laser-induced potential transients of an adatom-modified Pt(111) is illustrated in Figure 4 for the case of selenium and lead, because these cases provide representative examples for all studied adatoms. Results for the unmodified Pt(111) are included, for the sake of comparison.

In all cases, the potential transients are negative at sufficiently low potentials, indicating that interfacial water molecules exhibit a net orientation with their positive end (hydrogen) toward the metal (this point will be discussed in more detail below). As the potential is increased, the oxygen-toward-the-metal orientation is favored and the laser-induced potential transients become positive. The potential where the turnover of water molecules occurs can be identified with the potential of zero response ( $E_{\text{pZr}}$ ), which, in turn, corresponds to the pme of double-layer

(33) Batina, N.; Mccargar, J. W.; Salaita, G. N.; Lu, F.; Lagurendavidson, L.; Lin, C. H.; Hubbard, A. T. *Langmuir* **1989**, *5*, 123–128.

formation. Notably, the value of the pme is strongly dependent on the surface composition of the electrode. In the following section, the effect of the adatom coverage on the  $E_{\text{pzt}}$  will be analyzed.

#### 4. Discussion

The effect of the laser illumination on the surface of the electrode has been discussed in detail elsewhere.<sup>22–25</sup> Briefly, it can be assumed that the laser energy is immediately converted to heat at the surface of the electrode, and, therefore, the only effect caused by the laser is the increase of the interfacial temperature. Unfortunately, the exact temperature change induced by the laser pulse at the interface cannot be measured, because of the short time scale of the perturbation. However, it can be estimated through a simple heat transport model, giving  $\Delta T < 2 \text{ K}$  at  $t > 0.5 \mu\text{s}$ .<sup>25</sup>

As a result, the response of the interface toward the laser heating, under coulostatic conditions, is essentially given by the thermal coefficient of the potential drop across the double layer. Other possible effects—namely, the contributions due to changes in hydrogen coverage and the Soret or thermodiffusion potential—are very small under present experimental conditions.<sup>25</sup> To analyze this coefficient, it is convenient to consider the different contributions to the electrode potential in the absence of ion-specific adsorption:<sup>34–36</sup>

$$E^{\text{M}} = \frac{\Phi^{\text{M}}}{e} + \delta\chi^{\text{M}} - g^{\text{S}}(\text{dip}) + g(\text{ion}) + \text{constant} \quad (1)$$

where  $\Phi^{\text{M}}$  is the work function of the metal,  $\delta\chi^{\text{M}}$  is the modification of the surface potential of the metal (electron spillover) produced by the presence of the solvent,  $g^{\text{S}}(\text{dip})$  is the surface dipole associated with the excess of polarization of the solvent molecules at the metal/solution interface, and  $g(\text{ion})$  is the contribution of ions to the potential drop across the double layer. In concentrated electrolyte solutions, the potential drop across the diffuse layer can be neglected, and, hence,  $g(\text{ion})$  can be defined as  $g(\text{ion}) = \sigma/d\epsilon$ , where  $\sigma$  is the charge density on the metal,  $d$  is the thickness of the inner layer and  $\epsilon$  accounts for the distortional contribution to the effective permittivity of the inner layer that is due to molecular polarizability.<sup>37</sup> Derivation with temperature at constant charge gives the thermal coefficient of the double-layer potential:

$$\frac{dE^{\text{M}}}{dT} = \frac{1}{e} \frac{d\Phi^{\text{M}}}{dT} + \frac{d(\delta\chi^{\text{M}})}{dT} - \frac{d[g^{\text{S}}(\text{dip})]}{dT} \quad (2)$$

The constant in eq 1 does not vary with the temperature, because it includes only terms that correspond to the reference electrode, whose temperature is constant during the laser experiments. The temperature dependence of the ionic contribution,  $g(\text{ion})$ , can be considered to be zero, because  $d$  and  $\epsilon$  are molecular properties that should be only weakly dependent on the

temperature.<sup>30</sup> It should be emphasized that this assumption does not imply that the overall effective permittivity of the inner layer is independent of temperature; this quantity also contains contributions from the orientation of solvent molecules, which are dependent on the temperature, but these contributions are included in  $g^{\text{S}}(\text{dip})$ . The first term in the right-hand side of eq 2 corresponds to the thermal coefficient of the work function of the electrode, and it is usually very small (for a Pt(111) electrode,  $(d\Phi^{\text{M}}/dT)/e \approx -0.15 \text{ mV/K}$ ).<sup>38</sup> The second term is usually considered to be negligible.<sup>39</sup> In fact, these two terms constitute the entropy of metal electrons. In conclusion, the thermal coefficient of the double-layer potential is mainly determined by the temperature dependence of the dipole potential of the solvent network,  $d[g^{\text{S}}(\text{dip})]/dT$ .

Although  $(d\Phi^{\text{M}}/dT)$  is usually negative for most metals,<sup>40</sup> the value of  $d[g^{\text{S}}(\text{dip})]/dT$  can be positive or negative, depending on the sign of  $g^{\text{S}}(\text{dip})$ , in such a way that  $d[g^{\text{S}}(\text{dip})]/dT$  and  $g^{\text{S}}(\text{dip})$  will have opposite signs.<sup>41</sup> This is because an increase in the temperature will induce a disordering of the water network, thus decreasing the absolute value of  $g^{\text{S}}(\text{dip})$ . Therefore, when the water molecules are oriented with the positive end toward the metal, giving a positive contribution to the overall potential drop ( $g^{\text{S}}(\text{dip}) < 0$ ), the effect of an increase in temperature will be a decrease of this positive contribution, resulting in a negative contribution to  $dE^{\text{M}}/dT$ . Opposite arguments hold when the net orientation of the water network is with the oxygen toward the metal, ( $g^{\text{S}}(\text{dip}) > 0$ ), which results in positive potential coefficients. Between these situations, there is a potential value where  $d[g^{\text{S}}(\text{dip})]/dT = 0$ , which will correspond to the potential where  $g^{\text{S}}(\text{dip}) = 0$ . This potential will correspond to the maximum configurational entropy of the water adlayer. However, it is expected that, at strong negative or positive charge densities, the high electric field at the interface would induce the complete alignment of all dipoles, and, hence,  $g^{\text{S}}(\text{dip})$  will approach a saturation value and the value of  $d[g^{\text{S}}(\text{dip})]/dT$  will initially decrease and, finally, approach zero. However, for platinum electrodes, the situation where the absolute magnitude of  $d[g^{\text{S}}(\text{dip})]/dT$  starts to decrease with the increase of the electric field is difficult to attain, because of the high reactivity of platinum. In this regard, although a decrease of the magnitude of the laser-induced potential transients have been observed in several cases,<sup>22,23</sup> this behavior is more probably ascribable to specific adsorption phenomena.

To determine if the potential of zero response toward the laser heating ( $E_{\text{pzt}}$ ) corresponds to the state of maximum disorder or maximum order of the water adlayer, it is convenient to introduce the thermodynamic relationship between the thermal coefficient of the electrode potential and the entropy of formation of the double layer:<sup>21,27</sup>

$$\frac{dE^{\text{M}}}{dT} = -\left(\frac{\partial \Delta S_{\text{dl}}}{\partial q}\right)_T \quad (3)$$

where  $q$  is the charge density on the metal and  $\Delta S_{\text{dl}}$  is defined as the difference in the entropy of the constituents of the double

(34) Trasatti, S. In *Comprehensive Treatise of Electrochemistry*, Vol. 2; Bockris, J. O., Conway, B. E., Yeager, E., Eds.; Plenum: New York, 1980; pp 45–81.

(35) Trasatti, S.; Doubova, L. M. *J. Chem. Soc. Faraday Trans.* **1995**, *91*, 3311–25.

(36) Trasatti, S.; Lust, E. In *Modern Aspects of Electrochemistry*, Vol. 1; White, R. E., Bockris, J. O., Conway, B. E., Eds.; Kluwer Academic/Plenum Publishers: New York, 1999; pp 1–215.

(37) Fawcett, W. R. *Liquids, Solutions and Interface. From Classical Macroscopic Descriptions to Modern Microscopic Details*; Oxford University Press: New York, 2004.

(38) Kaack, M.; Fick, D. *Surf. Sci.* **1995**, *342*, 111–118.

(39) Guidelli, R.; Aloisi, G.; Leiva, E.; Schmickler, W. *J. Phys. Chem. B* **1988**, *92*, 6671–6675.

(40) Durakiewicz, T.; Arko, A. J.; Joyce, J. J.; Moore, D. P.; Halas, S. *Surf. Sci.* **2001**, *478*, 72–82.

(41) Trasatti, S. In *Modern Aspects of Electrochemistry*, Vol. 2; Conway, B. E., Bockris, J. O., Eds.; Plenum Press: New York, 1979; pp 81–205.

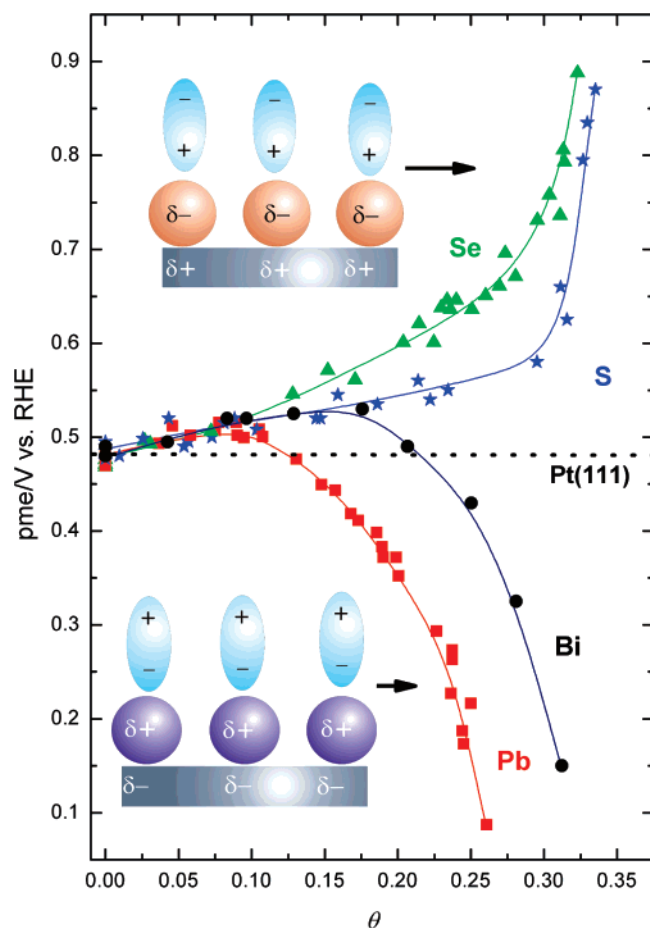


**Figure 5.** Potential of maximum entropy (pme), plotted as a function of the adatom coverage in a 0.1 M  $\text{KClO}_4$  + 1 mM  $\text{HClO}_4$  solution: Pb is represented by squares, Bi is represented by circles, Se is represented by triangles, and S is represented by stars. Illustrations show the schematic interpretation for the effect of the adatoms at high coverage on the potential transients. The dotted, zero-slope line corresponds to the averaged reference pme value of unmodified Pt(111).

layer when they are forming it and when they are present in the bulk of the adjoining phases.<sup>27</sup> The results presented here show that, at the  $E_{\text{pzc}}$ , transients change sign from negative to positive. In consequence, according to eq 3, the curve of  $\Delta S_{\text{dl}}$  vs  $q$  will show a relative maximum at this potential, and, hence, the  $E_{\text{pzc}}$  value can be identified as the pme of double-layer formation.

In conclusion, one significant parameter that can be obtained from the laser-induced potential transients is the value of the potential where the transient is zero ( $E_{\text{pzc}}$ ), because this potential can be identified with the pme. These potential values have been plotted as a function of the adatom coverage in Figure 5 for the four studied adatoms. Note that the introduction of a correction for the contribution of the thermodiffusion potential (approximately  $-0.048$  mV/K)<sup>23</sup> to the laser-pulsed measurements produces variations on the values of the pme below  $-10$  mV. Moreover, this contribution is independent of the nature of the electrode surface and, therefore, this small uncertainty does not affect the relative position of the pme values depicted in Figure 5. On the other hand, the introduction of a correction for the temperature coefficient of the work function of the bare Pt(111) electrode,  $(d\Phi^{\text{M}}/dT)/e \approx -0.15$  mV/K,<sup>38</sup> produces a displacement between the potential of water reorientation and the pme of  $<30$  mV toward lower potential values. Unfortu-

**Table 1.** Work Function ( $\Phi$ ) Values and Electronegativities ( $\chi$ ) of Elements Studied in the Present Work

element	work function, $\Phi$ (eV)	electronegativity, $\chi$
Bi	4.29 <sup>a</sup>	1.9 <sup>c</sup>
Pb	4.01 <sup>a</sup>	1.81 <sup>c</sup>
Se	5.9 <sup>b</sup>	2.55 <sup>c</sup>
S	6.2 <sup>d</sup>	2.58 <sup>c</sup>
Pt	5.40 <sup>a</sup>	2.2 <sup>c</sup>

<sup>a</sup> Data taken from Trasatti.<sup>42</sup> <sup>b</sup> Data taken from Williams and Polanco.<sup>43</sup> <sup>c</sup> Data taken from the *Handbook of Chemistry and Physics*.<sup>44</sup> <sup>d</sup> As estimated from  $\chi_{\text{S}}$ .<sup>45</sup>

nately, there currently are no experimental or theoretical data to take into account this effect in the presence of adatoms, but it is reasonable to assume that the correction also will be small.

The displacement of the pme at medium–high coverage of the adatoms seems to be correlated with the differences in work function values and electronegativities (see Table 1) between the adatom and the substrate. It can be observed that more-electropositive adatoms such as Bi and Pb, with work functions and electronegativities lower than that of platinum, shift the pme toward lower potential values, whereas more-electronegative adatoms such as Se and S displace the pme toward higher potential values. This effect can be explained by the fact that adsorbed adatoms will retain a partial charge, whose sign is dependent on the relative values of the electronegativity of the surface and the adatom, which induces the formation of a surface dipole that will affect the interaction of the water molecules with the surface (see the illustrative pictures in Figure 5). In other words, the adsorption of the adatoms would produce a marked shift on the work function (or potential of zero charge,  $E_{\text{pzc}}$ ) of the surface that will consequently displace the potential where water reorientation happens. Recall that this is, in fact, a simplified picture. The complete interpretation of the described effect should take into account, besides the electrostatic interaction, the existence of chemical interactions between water and the adatom, which will be certainly different, depending on the nature of the latter, and also the effect of adatoms on  $d\Phi^{\text{M}}/dT$  and  $d(\delta\chi^{\text{M}})/dT$ . However, the good correlation between the displacement of the pme and the work function (electronegativity) difference indicates that electrostatic interactions are the main cause for the displacement observed at high coverages in Figure 5.

The shift of the work function induced by deposition of foreign adatoms on a metal surface is a phenomenon that is already well-known in surface science, according to a well-established theory.<sup>46</sup> The results presented here provide evidence that similar trends are maintained in an electrochemical environment. In fact, this is expected from the relationship that exists between the  $E_{\text{pzc}}$  and the work function. The  $E_{\text{pzc}}$  can be obtained from eq 1 by considering  $g(\text{ion}) = 0$ :

$$E_{\text{pzc}}^{\text{M}} = \frac{\Phi^{\text{M}}}{e} + \delta\chi_{\text{pzc}}^{\text{M}} - g_{\text{pzc}}^{\text{S}}(\text{dip}) + \text{constant} \quad (4)$$

Therefore, it is expected that  $E_{\text{pzc}}$  will follow the variation in the work function, and, therefore, this variation will be reflected also on the pme. However, note that the variations of the work

(42) Trasatti, S. *J. Electroanal. Chem.* **1971**, *33*, 351.

(43) Williams, R. H.; Polanco, J. I. *J. Phys. C* **1974**, *7*, 2745–2759.

(44) *Handbook of Chemistry and Physics*; CRC Press: Boca Raton, FL, 1993.

(45) Gordy, W.; Thomas, W. J. *O. J. Chem. Phys.* **1956**, *24*, 439–444.

(46) Lang, N. D.; Williams, A. R. *Phys. Rev. B* **1978**, *18*, 616–636.



function by the adatom adsorption may be somewhat different to those produced on the  $E_{pzc}$ , because the terms  $\delta\chi_{pzc}^M$  and  $g_{pzc}^S(\text{dip})$  also may be modified by the adatom adsorption. In this respect, it is worth mentioning the classical work by Bange et al., who demonstrated that, in the presence of water-coadsorbed chloride, adsorption onto Ag(110) produced a non-linear variation of the  $E_{pzc}$  with the coverage, whereas a linear variation was observed on the work function.<sup>47</sup>

Work function measurements have shown that both Pb<sup>48</sup> and Bi<sup>49</sup> deposition markedly decreases the work function of a Pt(111) electrode, reaching a maximum decrease at full coverage of  $-1.5$  and  $-2.1$  eV, respectively. This is consistent with the direction of the change in the pme observed in electrochemical environment. However, the adsorption of sulfur at a saturation coverage of  $\theta_S = 0.33$  produces a negligible change of the work function of a Pt(111) electrode, and a maximum decrease of approximately  $-0.3$  eV is observed at  $\theta_S \approx 0.2$ .<sup>50,51</sup> These changes are not consistent with the trend of the pme observed in the present work. To reconcile both measurements, which have been obtained in very different environments, hydration effects should be taken into account. It is well-known that water adsorption on the bare Pt(111) produces a decrease of approximately  $-1$  eV in the work function, which indicates that  $g_{pzc}^S(\text{dip}) \sim 1$  eV.<sup>52</sup> In addition, it has been observed that the adsorption of species such as CO<sup>52</sup> or chlorine<sup>31</sup> markedly attenuates this effect. As a result, despite the fact that CO adsorption at near-saturation coverages produces a small effect on the work function of a bare Pt(111) electrode and chlorine adsorption produces an increase of  $\sim 0.5$  eV, the attenuation of the effect of water dosage results in an effective marked increase ( $\sim 1$  eV for CO and  $\sim 1.5$  eV for Cl) of the work function of a water-dosed Pt(111) electrode, that is expected to be reflected in the electrochemical environment as a marked positive shift of the  $E_{pzc}$ .<sup>53</sup> The same reasoning could be argued to explain an increase of the  $E_{pzc}$  of sulfur- and selenium-modified Pt(111) in an electrochemical environment.

As already stated, there is no direct measurement of  $E_{pzc}$  on adatom-modified platinum surfaces that can be used to corroborate the previously hypothesized relationship between the pme and the  $E_{pzc}$ . An alternative approach that can be used to estimate the effect of surface modification on  $E_{pzc}$  is based on the spectroscopic measurements of absorption bands of coadsorbed CO, which probes the local electronic state of the substrate. This indirect method, which has been validated under ultrahigh-vacuum (UHV) conditions,<sup>54</sup> has the advantage of its applicability under in situ conditions. However, it must be mentioned that this analysis should be performed with caution, because the frequency of the stretching of the CO band is critically dependent on the CO coverage, as a result of the strong effects of dipole-dipole coupling.<sup>55</sup> Consequently, even in the absence of electronic effects, it is expected that adatom

deposition will produce a lower frequency shift of the CO adsorption band, because of the diminishment of the CO coverage. In addition, the degree of intermixture between the adatom and the CO adlayer also is expected to exert an important role.

Studies with bismuth-modified Pt(111) electrodes<sup>56,57</sup> and lead-modified Pt(111) electrodes<sup>58</sup> have shown that these electropositive adatoms cause a clear displacement of the linear CO stretching adsorption band toward lower frequency values. These results also indicate that, in the electrochemical media, bismuth and lead deposition induces a decrease on the overall work function of the Pt(111), in agreement with the measured decrease of the pme of double-layer formation presented here. Conversely, more-electronegative adatoms (such as sulfur<sup>59</sup>) cause a higher-frequency shift of linear CO adsorption bands, in concordance with the increase of the pme observed from laser-pulsed experiments. Note that the deposition of selenium produces a red shift of the linear CO band,<sup>60</sup> although a blue shift would be expected from its electronegativity and work function values. However, in this case, the shift was interpreted as being due to the decrease of the CO-CO coupling associated with the decrease of the CO coverage caused by the adatoms, instead of being due to a true electronic effect.<sup>60</sup>

The explanation presented here for the behavior at medium-high coverages is also supported by results of previous studies on adatom deposition on stepped surfaces.<sup>61</sup> It has been shown that more-electronegative adatoms (such as S or Se) adsorb preferentially on the terrace sites, whereas more-electropositive modifiers (such as Bi, Cu, Sn, and Sb) decorate the step sites. This behavior was explained by the Smoluchowski effect or the creation of dipoles at step sites with an excess of negative charge at the bottom of the step.<sup>62</sup> Accordingly, electronegative adatoms would interact preferentially with the positively charged step edge sites, whereas electropositive adatoms would adsorb on the negatively charged step bottom sites. The present results of the variation of the pme at medium-high adatom coverages agree with the sign of the partial charge retained by the different adatoms inferred from the previous picture.

At low coverages, a small but reproducible increase of the pme with the coverage is observed in all cases, regardless of the nature of the adatom. In this regard, note that preliminary studies with other adatoms (Ge, Sn, As, and I) show the same behavior. Therefore, the observed trend at low coverages cannot be due to an electronic effect, because similar modifications are obtained with adatoms of very different chemical natures. A plausible explanation can be proposed considering the disrupting effect of adatom deposition on the structure of interfacial water. The optimization of hydrogen bonding is a key factor in determining the structure of the water network.<sup>28,63</sup> In the absence of an electric field, a net orientation of water

(47) Bange, K.; Straehler, B.; Sass, J. K.; Parsons, R. *J. Electroanal. Chem.* **1987**, *229*, 87–98.

(48) Mazinangokoudi, M.; Argile, C. *Surf. Sci.* **1992**, *262*, 307–317.

(49) Paffett, M. T.; Campbell, C. T.; Taylor, T. N. *J. Chem. Phys.* **1986**, *85*, 6176–6185.

(50) Kiskinova, M.; Szabo, A.; Yates, J. T. *J. Chem. Phys.* **1988**, *89*, 7599–7608.

(51) Billy, J.; Abon, M. *Surf. Sci.* **1984**, *146*, L525–L532.

(52) Kizhakevariam, N.; Jiang, X.; Weaver, M. J. *J. Chem. Phys.* **1994**, *100*, 6750–6764.

(53) Weaver, M. J. *Langmuir* **1998**, *14*, 3932–3936.

(54) Fukushima, T.; Song, M. B.; Ito, M. *Surf. Sci.* **2000**, *464*, 193–199.

(55) Chang, S.-C.; Weaver, M. J. *J. Chem. Phys.* **1990**, *92*, 4582.

(56) Chang, S.-C.; Weaver, M. J. *Surf. Sci.* **1991**, *241*, 11.

(57) Herrero, E.; Rodes, A.; Pérez, J. M.; Feliu, J. M.; Aldaz, A. *J. Electroanal. Chem.* **1995**, *393*, 87–96.

(58) Hoshi, N.; Bae, I. T.; Scherson, D. A. *J. Phys. Chem. B* **2000**, *104*, 6049–6052.

(59) Gracia, F. J.; Guerrero, S.; Wolf, E. E.; Miller, J. T.; Kropf, A. *J. Catal.* **2005**, *233*, 372–387.

(60) Herrero, E.; Rodes, A.; Pérez, J. M.; Feliu, J. M.; Aldaz, A. *J. Electroanal. Chem.* **1996**, *412*, 165–174.

(61) Herrero, E.; Climent, V.; Feliu, J. M. *Electrochem. Commun.* **2000**, *2*, 636–640.

(62) Smoluchowski, R. *Phys. Rev.* **1941**, *60*, 661–674.

(63) Thiel, P. A.; Madey, T. E. *Surf. Sci. Rep.* **1987**, *7*, 211–385.

molecules with the oxygen toward the metal is expected. This is the structure most commonly observed in UHV studies of water adsorption on metal surfaces, where the existence of an icelike bilayer with a preferential orientation of the molecules in the oxygen-down configuration is usually postulated.<sup>28,63</sup> The disruption of the water network as a consequence of adatom adsorption would facilitate the turnover of the water dipoles to the hydrogen-toward-the-metal orientation, which would occur at less-negative potentials (i.e., shifting the pme toward positive potentials). This disruption would be independent of the nature of the adatom, and, hence, it would be equivalent to a third body effect.

Three additional observations give support to the aforementioned hypothesis. First, the voltammetric behavior of adatom-modified Pt(111) in sulfuric acid shows that (bi)sulfate adsorption is shifted toward higher potential values by the adatom deposition at low coverages.<sup>14</sup> This effect has been ascribed to the fact that extended ordered (bi)sulfate adlayers are more stable than small ones, because of effective attractive lateral interactions.<sup>32</sup> The same argument can be applied to water adsorption; the disruption of the water adlayer decreases (in absolute value) its energy of adsorption. In addition, further support to the hypothesis of the disruption effect is obtained from experiments with Pt(111) stepped surfaces.<sup>24</sup> It is observed that the presence of steps induces the appearance of a second pme, which is associated with the local  $E_{pzc}$  of the steps. On the other hand, the pme that is associated with terrace sites is shifted toward higher potential values, indicating that the disruption of the bidimensional order of (111) terraces by the presence of steps, destabilizes a preferred structure of interfacial water with the oxygen toward the metal.

Finally, the effect of adatom deposition on Pt(111) stepped surfaces also agrees with the hypothesis given here. It is interesting to evaluate the effect of the Bi coverage on both pme values, which are ascribable to the step and terrace sites, respectively. Figure 6 shows results on the dependence of the pme associated with the terrace for the Bi coverage on Pt(997) and Pt(544) surfaces. In these surfaces, the bidimensional order of (111) terraces is disrupted by the presence of steps. In this figure, bismuth coverage has been evaluated from the degree of hydrogen blockage, assuming a saturation coverage of 0.33 in both the step sites and the terrace sites. That implicitly assumes that the same number of terrace and step sites are blocked by the adatom species; hence, this calculation should be considered to be only approximate.

The results in Figure 6 demonstrate that, in the absence of long-range order, the bismuth deposition does not increase the pme in any coverage range. At low coverages, where Bi decorates the step, the pme that is associated with the terrace remains essentially unaltered, while the signal that causes the appearance of the pme associated to the platinum step sites disappears. This behavior is explained by the fact that, within this coverage range, Bi deposition occurs preferentially on the step sites, with the terrace sites remaining unaffected; hence, the pme of the terraces remains unaltered. At higher coverages, the pme of the terraces decreases markedly, as observed for Bi-modified Pt(111) electrodes. As explained previously, this behavior is most likely due to the fact that deposition of bismuth on the terrace sites induces the formation of surface dipoles with the positive end oriented toward the solution. This

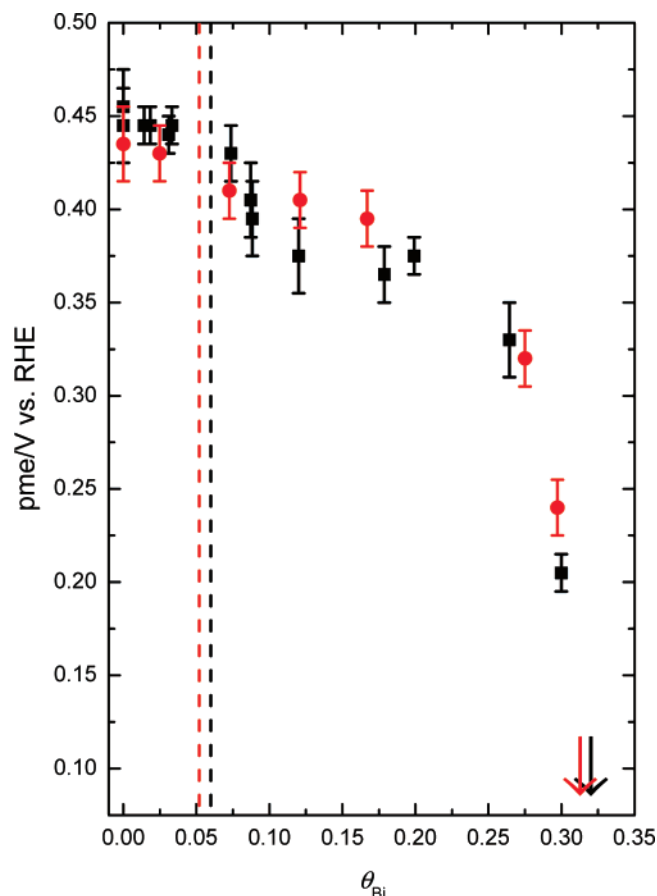


**Figure 6.** Potential of maximum entropy (pme) of Pt(997) (black squares) and Pt(544) (red circles) in 0.1 M HClO<sub>4</sub>, plotted as a function of the Bi coverage. Arrows indicate values of coverages where the pme was smaller than the lowest potential applicable before hydrogen evolution takes place (~0.1 V vs RHE). Vertical lines indicate the range of Bi coverages where the adatom adsorbs preferentially on the step site.

decreases the  $E_{pzc}$  of the terraces, and it is expected that the pme of the terraces would parallel this displacement.

## 5. Conclusions

Here, we have shown that a careful analysis of laser-induced potential transients of an adatom-modified, quasi-perfect Pt(111) electrode provides novel information on the behavior of water at electrified interfaces. Particularly, the potential where water reorientation occurs can be determined with high precision, and it is determined that its value is very sensitive to the surface composition. These results provide valuable information on the fundamental properties of bimetallic surfaces, which, in turn, are important for the understanding of the enhancement of the catalytic properties that are exhibited by these systems.

The evolution of the potential of water reorientation with the adatom coverage provides experimental evidence on the sign of the surface dipole induced by the adatom adsorption. The formation of this surface dipole results from the fact that more-electropositive (or more-electronegative) adatoms retain a partial positive (or negative) charge density. Consequently, local variations of the potential of zero charge ( $E_{pzc}$ ) values are induced by the adatom adsorption, which modifies the electronic properties of the substrate. The resulting effect on the electronic density on the substrate is important to understand the so-called “electronic or ligand effect in catalysis”.<sup>7,9</sup>

In addition, in some cases, the adsorbed adatoms provide suitable adsorption sites for the adsorption of one of the necessary reactants. This constitutes the basis of the bifunctional effect,<sup>1–3</sup> which has been shown to produce, in some cases, greatly improved catalytical activities. For example, it has been shown that the adsorption of oxygenated species on deposited adatoms at lower potentials than those on the platinum surface, produces a marked decrease of the onset potential for CO oxidation.<sup>57</sup> In this regard, it is observed that the potential where the adatom oxidation process occurs decreases as the adatom becomes more electropositive. In addition, the present results indicate that this process also may be associated with water reorientation, because it may be expected that the oxygen-toward-the-metal orientation may favor water dissociation to form oxygenated species on the surface.

Finally, the comparison of the effect of adatom deposition on a virtually defect-free Pt(111) electrode and on Pt(111) stepped surfaces allows us to conclude that water–metal interactions are very sensitive to long-range order. The adatom deposition involves a noticeable disruption of the structure of interfacial water, which is almost independent of the nature of the adatom, and can be then considered as a third body effect.

The consequent decrease on the strength of water adsorption is expected to facilitate the adsorption of species whose interaction with the platinum surface is weak (such as N<sub>2</sub>O<sup>64</sup> or peroxydisulfate<sup>20</sup> molecules). In these cases, the reaction rate is usually determined by the adsorption step; hence, the increase in the coverage of these species is expected to produce a proportional increase in the reaction rate.

In conclusion, the new information about the interaction of solvent molecules with the electrode surface obtained from nanosecond-laser-pulsed experiments has been demonstrated to be valuable, in regard to providing a deeper understanding of some general trends that are observed in electrocatalysis.

**Acknowledgment.** Financial support from the MEC (Spain), through Project No. CTQ 2006-04071/BQU, is gratefully acknowledged. N.G. thanks the MEC (Spain) for the award of a FPU grant. V.C. acknowledges financial support from the MEC, the Generalitat Valenciana, and the University of Alicante (under the Ramon y Cajal).

JA0761481

(64) Attard, G. A.; Bersier, P. M. *J. Electroanal. Chem.* **1995**, *383*, 199–201.